

Effect of covariance between ablation and snow water equivalent on depletion of snow-covered area in a forest

D. A. Faria,¹ J. W. Pomeroy^{2*} and R. L. H. Essery¹

¹*Division of Hydrology, University of Saskatchewan, Saskatoon, Saskatchewan, S7N 5A9, Canada*

²*Centre for Glaciology, Institute of Geography and Earth Sciences, University of Wales, Aberystwyth, Wales SY23 3DB, UK*

Abstract:

The influence of the spatial distribution of snow water equivalent and covariance between spatial distributions of ablation and snow water equivalent on depletion of snowcover was investigated in the boreal forest of central Saskatchewan, Canada. Changes in the spatial distributions of snow water equivalent were measured before and during melt in five stands, ranked by canopy density as: black spruce, jack pine, mixed wood, burned and recent clear-cut. The pre-melt frequency distribution of snow water equivalent within forest stands was found to fit a log-normal distribution. Higher variability in snow water equivalent resulted in earlier exposure of ground under spatially uniform melt simulations, confirming the previous findings of others for open environments. The spatial distribution of daily ablation within stands was found, however, to be correlated inversely to the distribution of snow water equivalent. This negative covariance between snow water equivalent and ablation further accelerated snow cover depletion. The combined acceleration as a result of variance of snow water equivalent and covariance with ablation was greatest in mixed-wood stands and smallest in burned and spruce stands. Simulations that included the within-stand covariance of ablation and snow water equivalent showed improved fit with measured data over those that only considered the effect of the distribution of snow water equivalent on snow-cover depletion. Copyright © 2000 John Wiley & Sons, Ltd.

KEY WORDS forest hydrology; boreal forest; snow accumulation; snowmelt; snow-cover depletion; snow covered area; ablation

INTRODUCTION

Depletion of snow-covered area (SCA) during melt in forest environments affects areal albedo, subcanopy energy balance, soil moisture recharge and runoff generation. Snow-covered area is also used to index snow water equivalent (SWE) at large scales (Cline *et al.*, 1998; Martinec and Rango, 1991; Martinec *et al.*, 1991). Buttle and McDonnell (1987) noted that the rate of depletion of snow cover in forest stands can be influenced by the variabilities in SWE or melt rate or some combination of the two. Shook (1995), Donald *et al.* (1995) and Pomeroy *et al.* (1998a) showed that the distribution of SWE controls the rate of snow-cover depletion in open environments.

It is important to distinguish the effect of the scale of observation when considering factors that influence snow-cove depletion. In the boreal forest, it is well-established that at and above the stand-scale, pre-melt SWE (Pomeroy and Gray, 1995) and melt rate (Metcalf and Buttle, 1995, 1998; Davis *et al.*, 1997; Pomeroy and Granger, 1997) decrease with increasing canopy density. At these large scales, open canopies not only intercept less snow (Pomeroy *et al.*, 1998b) but attenuate less radiation (Ni *et al.*, 1997) than do dense coniferous canopies.

* Correspondence to: J. W. Pomeroy, Centre for Glaciology, Institute of Geography and Earth Sciences, University of Wales, Aberystwyth, Wales SY23 3DB, UK. E-mail: John.Pomeroy@aber.ac.uk

At finer scales, Woo and Steer (1986), Jones (1987), Sturm (1992), Pomeroy and Goodison (1997) and Pomeroy *et al.* (1999) showed that SWE increases with distance from evergreen tree trunks (up to a distance of roughly 3 m) in cold-climate forests (Figure 1). These small-scale observations concur with the trend showed by stand-scale observations of SWE as described above.

Within a stand, the positive covariance between SWE and melt rate observed at stand scales, may not apply. Physical considerations suggest that absorption of short-wave radiation by trunks and branches and its redistribution as long-wave energy to adjacent snow can affect ablation patterns (Verry *et al.*, 1983; Golding and Swanson, 1986). Shallower forest snow may also have a lower albedo (Davis *et al.*, 1997). Shook and Gray (1997), Takahara and Higuchi (1985) and Weisman (1977) demonstrated that the contribution of additional advected energy from snow-free surfaces during snowmelt decreases with distance from the snow-cover edge. If it is presumed that SWE increases with distance from trunks, then either radiation or advection from trunks or bare ground surrounding trunks could produce an inverse association between SWE and melt energy. Jones (1987) developed a regression equation based on extensive field data that described the influence of proximity to, and size of conifers on SWE. Snow water equivalent declined with proximity to trunks. The relationship persisted throughout melt, suggesting that melt rates were not significantly higher for greater SWE. Buttle and McDonnell (1987) found that a relationship (admittedly arbitrary) in which melt rate decreased with increasing SWE performed well in predicting snow-cover depletion in certain forest environments.

Shook (1995) concluded that the distribution of SWE affects the rate of snow-cover depletion in open areas but the above review suggests that a covariance between SWE and melt energy may confound such direct relationships in the forest. The objectives of this paper therefore are to establish:

- (1) what association exists between SWE and ablation within a forest stand;
- (2) whether the association can be attributed to canopy characteristics;



Figure 1. Increase in SWE and depth with distance from the central trunk of a white spruce tree in a mixed-wood aspen/spruce stand, Prince Albert National Park, Saskatchewan. Showing measurements discussed in more detail by Pomeroy and Goodison (1997)

- (3) how the within-stand relationship between SWE and ablation affects the depletion of SCA at both small and large scales in boreal forests.

EXPERIMENT

The study sites were located in central Saskatchewan, Canada (54°N , 106°W), in the southern, mid-continental boreal forest (Figure 2). Five boreal environments were examined: within Prince Albert National Park, a mature black spruce (Spruce), a mature jack pine (Pine), and a mature mixed wood of mostly aspen with some white spruce (Mixed); in the Northern Provincial Forest, a recent complete burn of a mature black spruce to standing charred trunks (Burn), and a recent large clear-cut replanted to white spruce with some managed aspen regrowth (Clear-cut).

Effective winter leaf area index (LAI') was measured as the horizontal area of winter leaf + stem extinguishing incoming solar radiation per unit area of ground using a LI-COR LAI2000 optical meter (Table I). Basal area and stem density for three sites (Mixed, Pine and Spruce) were measured in 1994 (Halliwell and Apps, 1997). The distribution of SWE was sampled before and during the 1997 spring snowmelt, along fixed, 100 m long, north–south transect lines, one line at each study site. Location of sample points with respect to distance from trees was unbiased, with some points directly under tree crowns adjacent to trunks and others under the canopy gaps. Each sample consisted of snow depth measured with a ruler every metre along a transect, and snow density measured with an ESC-30, snow pit density profile or a radiological densitometer every 10 m (Pomeroy and Gray, 1995). Daily mean areal snowmelt rates were estimated from changes in mean SWE over the transect.

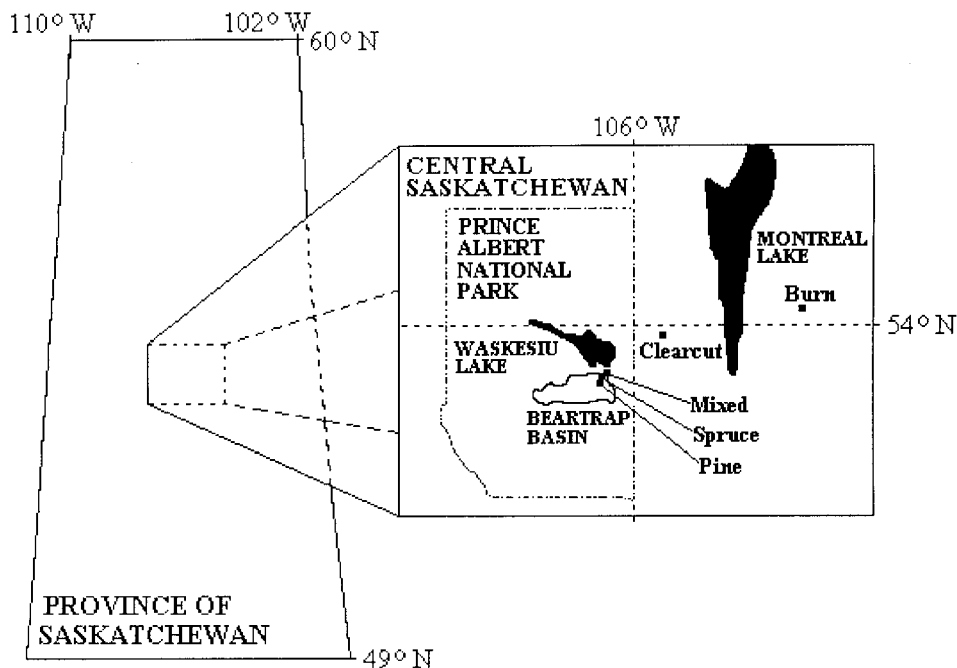


Figure 2. Location of five study sites in central Saskatchewan. Three mature stands are near the outlet of Beartrap Creek basin, with the other two sites east of Prince Albert National Park

Table I. Canopy structure (effective leaf area index, LAI', maximum tree height, basal area and stem density) and initial SWE distributions sampled at five study sites. Basal area and stem density are from 1994 forest mensuration (Halliwell and Apps, 1997)

Site name	Spruce	Pine	Mixed	Burned	Clear-cut
LAI' (m ² m ⁻²)	4.1	2.2	0.7	0.23	0.06
Tree height (max.)	15 m	22 m	26 m	10 m	1 m
Basal area (m ² ha ⁻¹)	45.9	40.2	32.9		
Stem density (ha ⁻¹)	6284	1470	1026		
Sample date	25 March	27 March	25 March	26 March	24 March
Mean of SWE	58 mm	49 mm	88 mm	74 mm	89 mm
CV of SWE	0.19	0.18	0.16	0.09	0.19

For modelling ablation, snowmelt energy was estimated from changes in point SWE estimates from snow-depth measurements made using an ultrasonic depth gauge on a half-hourly basis. When snow cover under this gauge was depleted, half-hourly snowmelt energy fluxes were estimated from measured subcanopy net radiation less ground heat flux. Subcanopy net radiation was measured using a Delta-T tube net radiometer at the Mixed and Pine (1-m height), and a REBS Q7 net radiometer at the Burn and Spruce (1-m height) and Clear-cut (4-m height). Digital photographs of a small area of forest floor were taken with a Logitech 'Fotoman' camera at two of the sites (Pine and Burn) during melt.

METHODOLOGICAL APPROACH

Faria (1998) found only a small spatial covariance (< 1.2 mm of SWE) between d_s and ρ_s during melt at these sites. It was therefore assumed that SWE (mm) at each sample point could be estimated as

$$SWE = d_s \times \bar{\rho}_s \quad (1)$$

where d_s is the point snow depth (m) and $\bar{\rho}_s$ is the mean snow density (kg m⁻³). Shook (1995) found that measurements of SWE in open environments fit the two-parameter log-normal distribution, for which the probability density function is

$$p(SWE) = \frac{1}{\sqrt{2\pi}S_y SWE} \exp\left(-\frac{(y - \bar{y})^2}{2S_y^2}\right) \quad (2)$$

where $y = \ln(SWE)$. The mean \bar{y} and standard deviation S_y of y are given by

$$\bar{y} = \frac{1}{2} \ln\left(\frac{\overline{SWE^2}}{1 + CV^2}\right) \quad (3)$$

and

$$S_y = \sqrt{\ln(1 + CV^2)} \quad (4)$$

for a set of SWE measurements with mean \overline{SWE} and coefficient of variation CV .

Equation (2) can be integrated and expressed by the linear form,

$$SWE = \overline{SWE}(1 + KCV) \quad (5)$$

where K is the frequency factor given by Chow (1954) as

$$K = \frac{1}{CV} \left[\exp \left(S_y K_y - \frac{S_y^2}{2} \right) - 1 \right] \tag{6}$$

where the transformed frequency factor K_y equals $(y - \bar{y})/S_y$. Note that natural values of K and SWE should be used in Equation (5). If the underlying distribution is log-normal, plotting sampled values of SWE against K should give a straight line with slope equal to the standard deviation of SWE and intercept ($K = 0$) equal to \overline{SWE} . Given that the cumulative probability, P , of SWE and K_y are equal, for each sample of N observations, ranked by r in increasing order of magnitude, P can be related to K_y by inverting the cumulative normal distribution, where

$$P(SWE) = \frac{r}{N + 1} = \frac{1}{\sqrt{2\pi}} \int_{-\infty}^{K_y} e^{-K_y^2/2} dK_y \tag{7}$$

The exceedance probability for the minimum K value, K_{\min} , is equal to SCA.

The distribution of ablation from the snow cover was calculated between consecutive surveys by assuming that sample points maintained their rank and K values. Ablation at a point was presumed equal to applied melt at that point, M . Dividing M by the mean applied melt, \bar{m} , over the snow cover (excluding $SWE = 0$ observations) gave normalized applied melt. As the snow cover depleted, the number of points with snow decreased. To describe melt rate as a function of position in the remaining SWE distribution, observed M values ($SWE > 0$) were assigned a rank, r , in increasing order of K magnitude. Pre-melt K values for rank r , $K_i(r)$, were then assigned to all points of the same rank. To examine the relationship between ablation and SWE, $M(r)$ was related to $K_i(r)$ by

$$\frac{M(r)}{\bar{m}} = aK_i(r) + b \tag{8}$$

where a and b are fitted parameters. This was done for each site by averaging $M(r)/\bar{m}$ for intervals of $K_i(r)$, and fitting a linear function (Equation 8) to the averaged values.

Equation (8) was used with \overline{SWE} and CV just prior to active melt to calculate relationships between SCA and melt using the calculation scheme Simulation of Distributed-melt Effects on Snow-cover Depletion Curves. The SDMESDC scheme presumes that the applied melt rate, M , is some function, $q(K)$, where

$$M = \frac{dSWE}{dt} = -q(K) \tag{9}$$

so that SWE from some K after some time t is

$$SWE(K, t) = \overline{SWE}_i(1 + KCV_i) - q(K)t \tag{10}$$

where the subscript i denotes a pre-melt value. All points with initial $K < K_{\min}(t)$ will be snow-free by time t , where K_{\min} is the solution at

$$\overline{SWE}_i(1 + K_{\min} CV_i) - q(K_{\min})t = 0 \tag{11}$$

The SCA and mean SWE at time t are given by

$$SCA(t) = \int_{q(K_{\min})t}^{\infty} p(SWE) dSWE \tag{12}$$

and

$$\overline{SWE}(t) = \int_{q(K_{\min})t}^{\infty} [SWE - q(K)t]p(SWE) dSWE \quad (13)$$

where $p(SWE)$ is the probability density (Equation 2) of the SWE distribution just prior to active melt, and the lower limit of the integral at time t is the applied melt at K_{\min} (Equation 11). Changes in mean SWE reflect 'resultant melt' (per unit area of forest floor). Measurements of resultant melt were obtained from survey estimates of mean areal SWE and from interpolations between surveys using half-hourly measurements of point ablation or observed subcanopy melt energy.

RESULTS

Figure 3 shows an example of the sequence from pre-melt to active melt for the Pine site. Between pre-melt and active melt there was a period of both melt and snowfall, which complicated the analysis. For this reason, the SWE distribution at the start of active melt was used in calculating SCA depletion. The log-normal distribution was found to be a good approximation for pre-melt forest snow surveys of SWE, as shown in Figure 4 for the Pine stand. Table I outlines the log-normal distribution parameters for the initial samples taken at all sites in late March prior to appreciable melt. Except for the Clear-cut stand where wind redistribution of snow is a factor (Pomeroy and Gray, 1995), the CV within a stand decreased with decreasing canopy density.

Figure 5 shows an example of distributions of SWE before and during active melt in the Pine stand. Mean and CV for distributions from all sites just before active melt are shown in Table II. Ablation for a given K is the reduction in SWE. Increases in K_{\min} reflect the reduction in SCA. Initial distributions fit the log-normal distribution, but progressively larger deviations from the initial log-normal distribution developed during melt. The downward curvature developed for shallower depths of the distribution. This deviation suggests a covariance in which greater ablation is associated with smaller SWE.

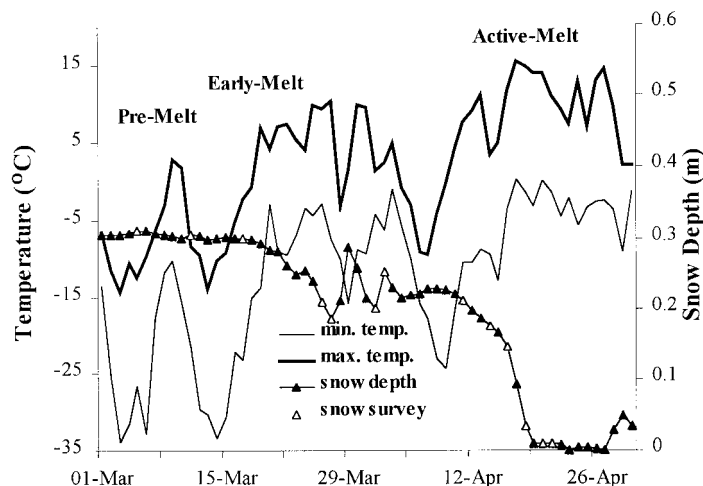


Figure 3. Timing of melt sequence for the Pine stand in spring 1997. Daily minimum and maximum subcanopy air temperatures (1-m height), and daily mean of half-hourly point snow-depth measurements are shown. Snowfall, melt and snow surveys are indicated on the snow depth time-series, which is divided into pre-melt, early-melt and active-melt periods

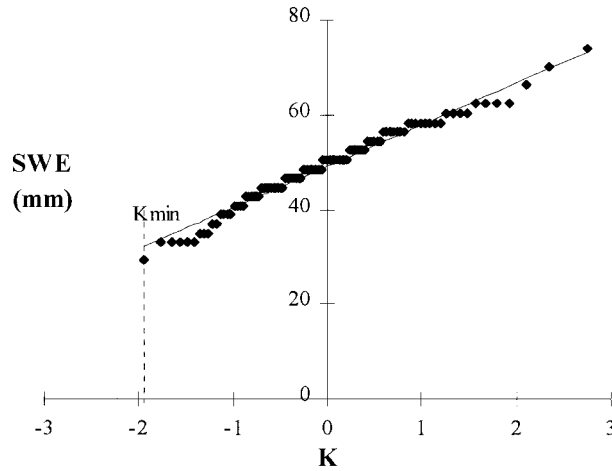


Figure 4. Example of sampled pre-melt SWE distribution in the pine stand and a fitted log-normal distribution (27 March 1997)

To examine the association between SWE and ablation, further observations and physical considerations were used. Sequential photographs of areal snow-cover extent taken during melt (Figure 6) show depletion of SCA spreading outwards from trunks. As seen in Figure 6, the pattern is apparent for both the Pine canopy, for which snow interception reduced SWE near trunks, and the Burned stand, for which interception was small. The SCA depletion patterns observed in the pine could be the result of variable SWE, variable melt or a covariance of the two, the pattern observed in the Burned stand probably is dominated by increasing melt energy with proximity to trunks. Such a pattern might be consistent with energy redistribution processes, whereby melt energy, excess to the subcanopy ‘average’, is radiated or advected from tree trunks. Fitted relationships between K and $M(r)/\bar{M}$ (Equation (8), before conversion of K to $K_i(r)$) were, however, in poor agreement for $SCA < 1$, suggesting that position with respect to trunks alone was not governing the correlation between the spatial distributions of applied melt and SWE (Faria, 1998). Analysis therefore

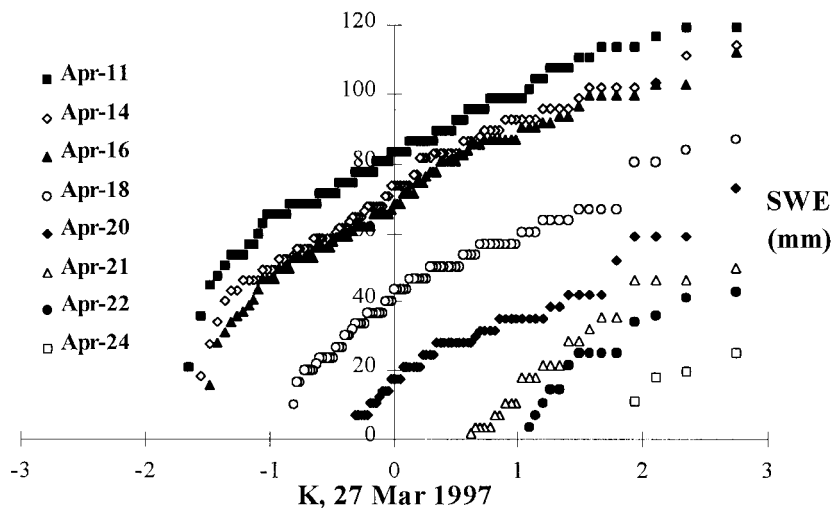


Figure 5. Active-melt distributions of SWE in the Pine stand, April 1997

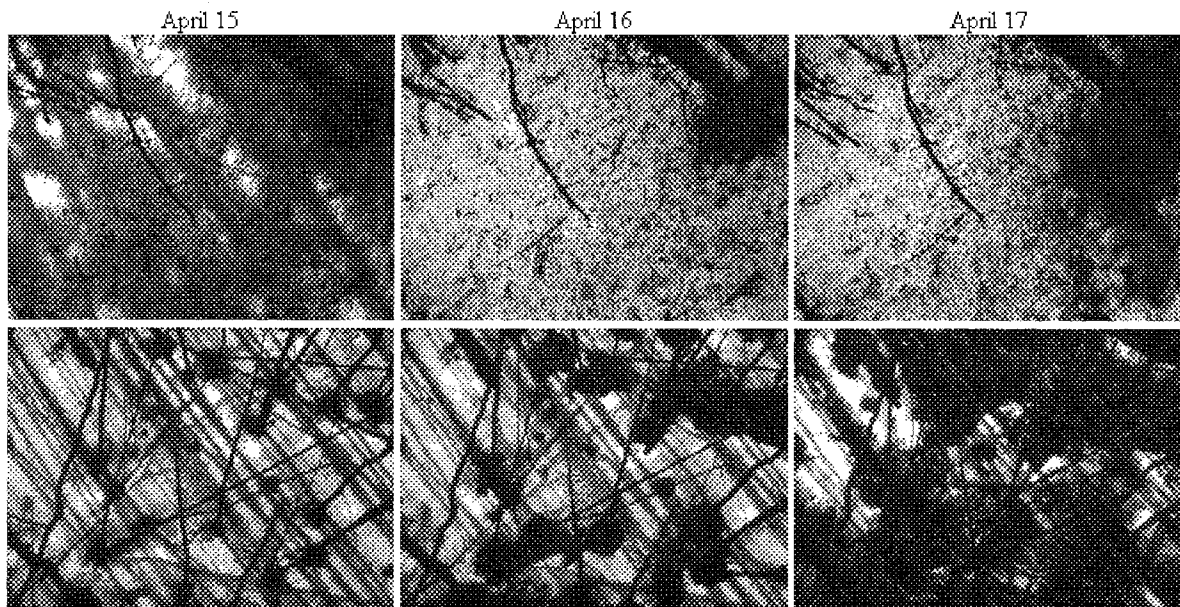


Figure 6. Sequential photographs (24-h intervals), showing initial ablation of the shallow snow near trunks (top 3, Pine stand; bottom 3, Burned stand). Digital cameras (Fotoman) were positioned on towers at these sites: Pine, 5-m height; Burned, 11-m height

concentrated on relationships between $K_i(r)$ and $M(r)/\bar{M}$, presuming that the SWE distribution was the relevant parameter in the statistical relationship.

Figure 7 shows an example of averaged $M(r)/\bar{M}$ against $K_i(r)$ for the melt periods at the Pine stand site (Figure 5) and the best-fit line (Equation 8). Values of the fitted parameters a and b (Equation 8) are given in Table II for all five sites. The slope (a), which describes the covariance between SWE and ablation, varied with canopy density. Coefficient a was largest for the low density, primarily deciduous stands (Mixed, Burn

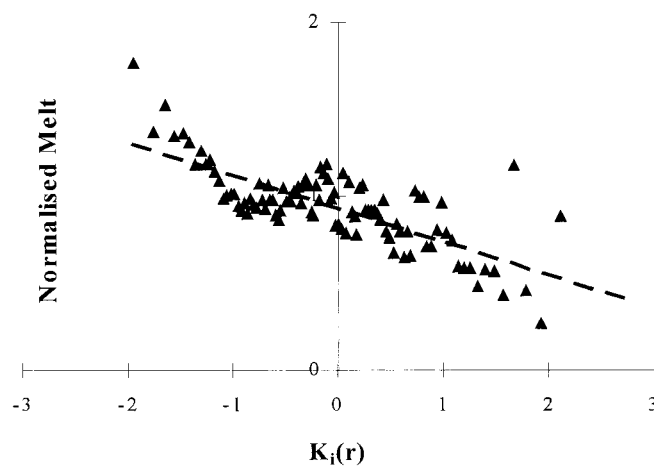


Figure 7. Distribution of normalized melt, given as a linear function of the pre-melt distribution frequency factor. Average values and linear fit are shown

Table II. Distribution parameters for covariance of ablation and SWE, and SWE distribution just prior to active melt

Site/function	Spruce	Pine	Mixed	Burned	Clear-cut	Uniform melt
a (slope)	- 0.12	- 0.19	- 0.29	- 0.25	- 0.3	0
b (intercept)	1.0	0.9	0.9	1.0	1.0	1.0
R^2 (regression)	0.37	0.58	0.72	0.91	0.59	
Sample date	11 April	11 April	11 April	10 April	10 April	
Mean of SWE	72 mm	80 mm	102 mm	85 mm	104 mm	90 mm
CV of SWE	0.24	0.28	0.26	0.13	0.21	0.22

and Clear-cut) and smallest for the high density, coniferous stands (Spruce and Pine). The intercept b is 1 when the mean melt rate coincides with mean SWE. This occurred in the Spruce, Burn and Clear-cut stands but not the Pine and Mixed stands, where b was 0.9. Results for the Mixed and Clear-cut stands were very similar, interestingly both stands were composed of aspen and spruce, but the Mixed canopy was an order of magnitude taller and denser than that at the Clear-cut.

The effect of covariance between SWE and applied melt within stands on snow-cover depletion was calculated using SDMESDC. The programme was initialized with the fitted values of a and b , measured values of the initial SWE distribution at the initiation of active melt (Table II) and estimated mean applied melt. Figure 8a shows results of the simulation of the SCA and fraction of snowmelt per unit area of ground (resultant-melt fraction), for the measured covariance at the five study sites, and for no covariance (variation in SWE alone) with the CV equal to the areal mean for all stands of 0.22. It is seen that increased covariance acts to accelerate SCA depletion. Figure 8b shows simulation results using measured CV and covariance. The combined effects on SCA depletion of covariance and CV are somewhat counteracted because covariance and CV are complementary, with the former increasing and the latter decreasing with increasing canopy density. As a result, SCA depletion is accelerated the most at the Mixed (moderate degrees of both CV and covariance) and least at the Burned and Spruce stands because of low CV (Burn) and low covariance (Spruce), respectively.

Figure 9 'scales-up' the results by showing the stand-scale simulated depletion of SCA as a function of time for five stands, using measured stand CV and covariance and stand-scale resultant melt rate. At the stand scale, the rate of depletion decreases with increasing canopy density.

To illustrate the change in snow-cover depletion simulation as a result of covariance between ablation and SWE, the SDMESDC simulations of SCA, such as shown in Figure 9, were compared with simulations of SCA depletion due only to the distribution of SWE (again using SDMESDC) and to the SCA measured with the transect surveys (Figure 10). Inclusion of a covariance between melt and SWE improved the simulations compared with the simulation using SWE distribution alone (Figure 10).

DISCUSSION

The results have shown that a covariance between melt and SWE accelerates the depletion of SCA in forest beyond that introduced by the distribution of SWE alone. At the stand scale, the covariance increases with decreasing CV , and so the variability amongst stands in SCA depletion is reduced from that due to either CV or covariance in isolation. When the mean melt rate is applied to drive melt simulations, the variation in melt rate amongst stands is apparent as another important variable in calculating forest snow-cover depletion at large scales.

Interpretation of these results to provide physical mechanisms behind the covariance of SWE and melt is problematic and based upon the acceptance of two key assumptions:

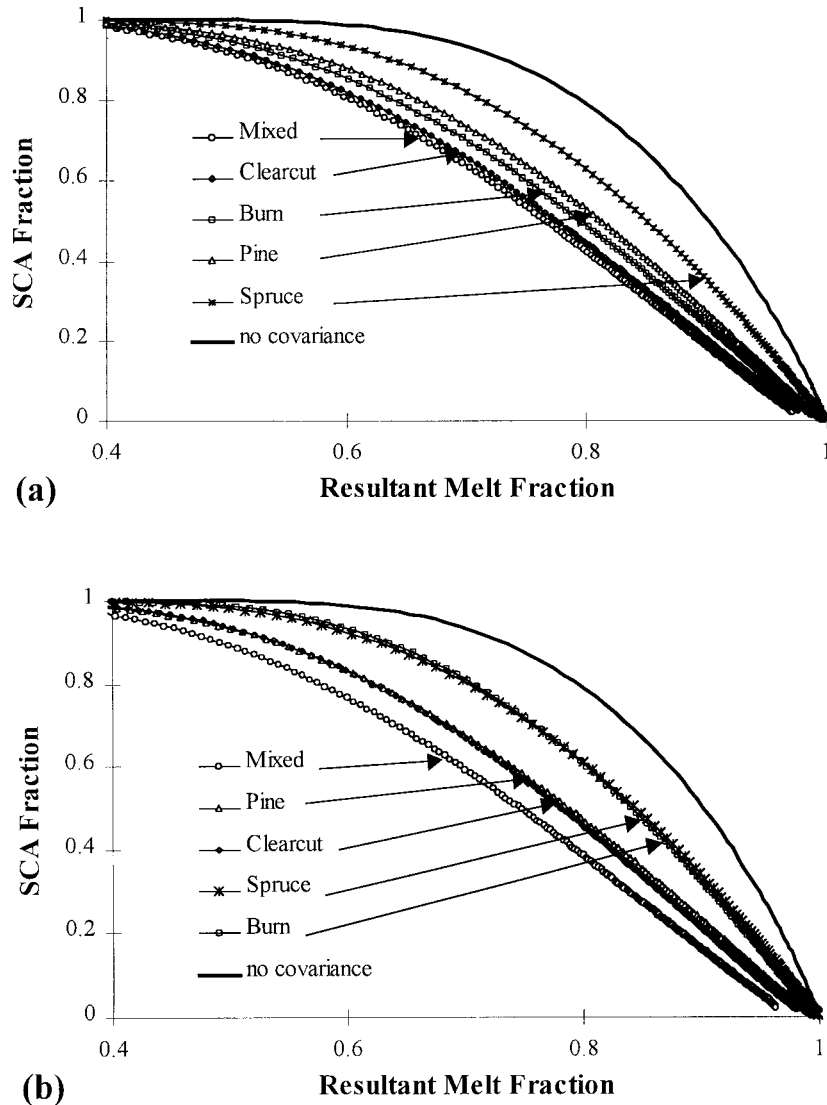


Figure 8. Simulated snow-cover depletion curves: (a) using $CV = 0.22$ and observed within-stand covariance between melt and SWE; and (b) using measured within-stand CV and covariance between melt and SWE. Simulation with no covariance ($CV = 0.22$) is shown for comparison

- (1) SWE rank and position of rank (as described by K) with respect to the canopy and trunks do not change during melt (probably true unless the cumulative variation in melt overwhelms the initial variation in SWE);
- (2) SWE increases with distance from trunks (probably true for conifers, not for deciduous).

For the case where both assumptions are true then depletion will proceed from trunks outward, from the lowest to the highest SWE rank. The SWE rank is therefore a function of distance from the trunk at the beginning of melt and distance from the snow-cover edge during melt. It is conceivable that a combination of

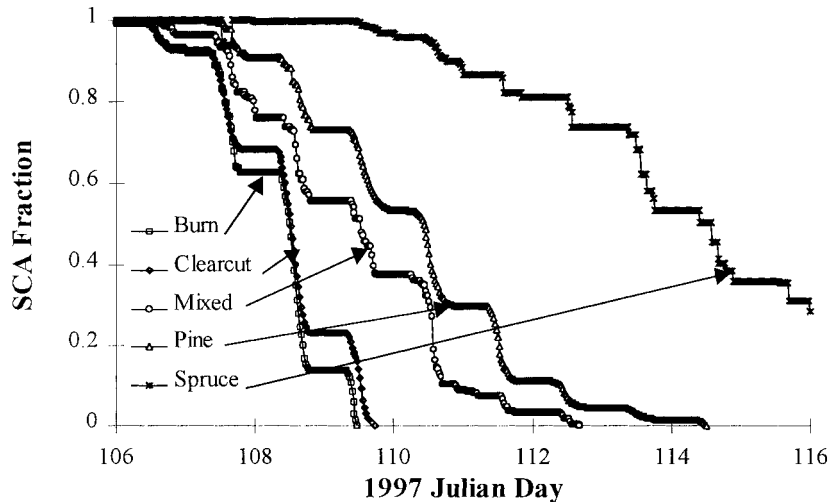


Figure 9. Simulated stand-scale snow-cover depletion sequence using measured within-stand CV and covariance between melt and SWE, and measured stand-scale melt rate

radiation from trunks and advection from trunks and bare ground could cause the covariance of melt and SWE in this case.

The case outlined above, however, is not generally applicable to all the stands for which a covariance was measured (e.g. Burn and Clear-cut). Without requiring any assumption about spatial position of ranks, it is clear that higher melt is associated with smaller SWE and therefore shallower depths for all stands studied. Possible mechanisms for accelerated melt with shallower snow are:

- (1) lower snow albedo owing to greater leaf litter concentration or influence of underlying forest floor on albedo as snow becomes more shallow;
- (2) increased advection of energy from exposed plants (bushes, stems and trunks) as snow becomes more shallow.

The effectiveness of both mechanisms should increase with increasing incident solar radiation, in accordance with the observed inverse relationship between covariance and effective leaf area. Through lack of direct physical observations, this discussion cannot contribute to the conclusions of this paper but perhaps can guide the formation of hypotheses for future studies of snowmelt energetics under forest canopies and elsewhere in complex environments.

CONCLUSIONS

- (1) Pre-melt variance of SWE within boreal forest stands increases with increasing canopy density; an exception was for clear-cuts, which had relatively high variance in SWE.
- (2) Melt rate is inversely correlated with SWE within boreal forest stands.
- (3) The covariance of melt rate with SWE increases with decreasing canopy density.
- (4) The covariance between melt rate and SWE results in an accelerated depletion of SCA within a stand, compared with depletion rates resulting from variation in SWE alone.
- (5) Because of the combined effects of variance in SWE and covariance between melt rate and SWE, the greatest acceleration of snow-cover depletion occurs within a medium-density mixed-wood stand,

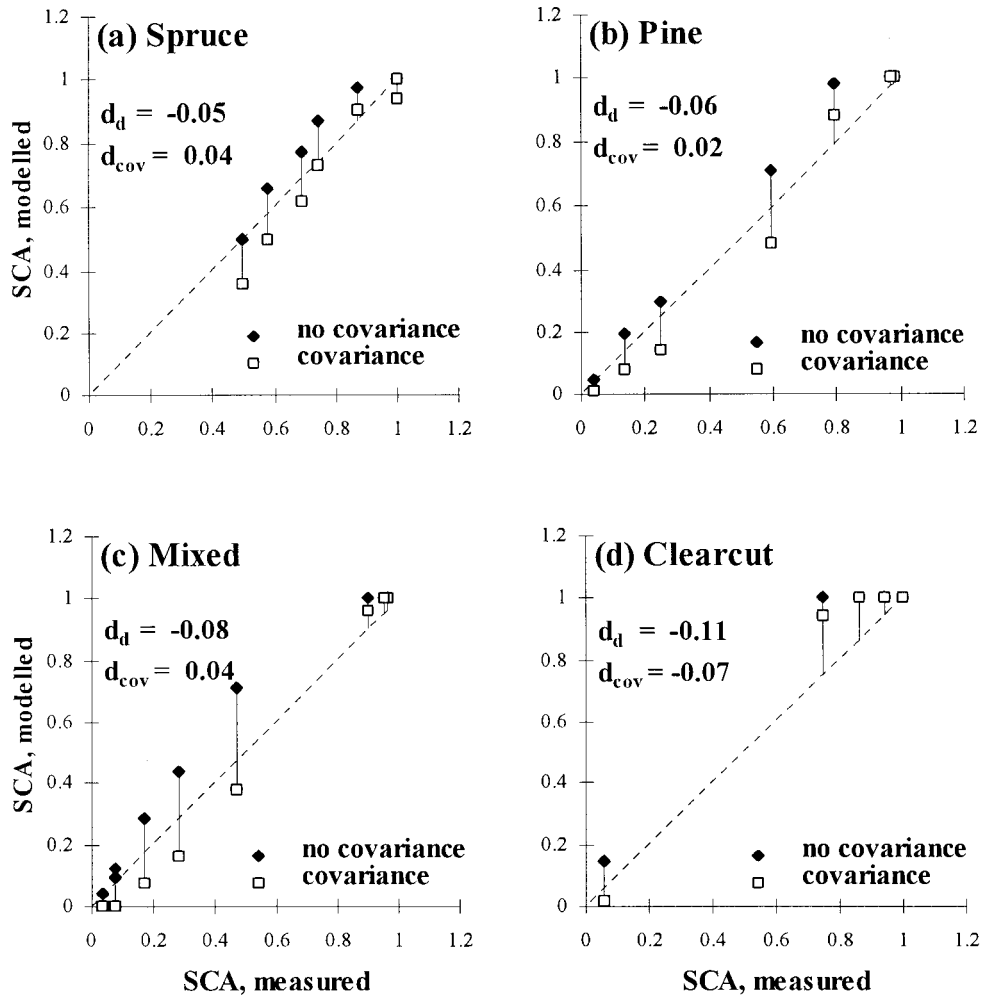


Figure 10. Comparison of modelled snow-covered area (SCA) with SCA measured along transects at four sites. The mean of measured – modelled SCA for simulations with and without covariance between melt and SWE is given as d_{cov} and d_d respectively

moderate acceleration within medium density pine and open clear-cut stands and least acceleration within low density burned and high density black spruce stands.

- (6) To calculate areal depletion of snow cover at the stand scale, it is necessary to consider the variation of stand-scale snow accumulation and melt energetics together with the within-stand variation of SWE distribution and the within-stand covariance between melt and SWE.

ACKNOWLEDGEMENTS

The authors wish to acknowledge funding from the Climate Research Network — Land Surface Processes Node; Mackenzie GEWEX Study; Natural Sciences and Engineering Research Council of Canada; Prince Albert Model Forest; Prince Albert National Park and National Hydrology Research Institute, Environment Canada. RE thanks the Hadley Centre, UK Meteorological Office for leave to conduct this work. The assistance of Dell Bayne and Newell Hedstrom in the field and advice of Dr Kevin Shook were

invaluable to completing this study. Professor Don Gray and two anonymous reviewers provided helpful comments on the manuscript.

REFERENCES

- Buttle JM, McDonnell JJ. 1987. Modelling the areal depletion of snowcover in a forested catchment. *Journal of Hydrology* **90**: 43–60.
- Chow VT. 1954. The log-probability law and its engineering applications. *Proceedings of the American Society of Civil Engineers* **80**(536): 1–25.
- Cline DW, Bales RC, Dozier J. 1998. Estimating the spatial distribution of snow in mountain basins using remote sensing and energy balance modelling. *Water Resources Research* **34**(5): 1275–1285.
- Davis RE, Hardy JP, Ni W, Woodcock C, McKenzie JC, Jordan R, Li X. 1997. Variation of snow cover ablation in the boreal forest: a sensitivity study on the effects of conifer canopy. *Journal of Geophysical Research* **102**: 29389–29395.
- Donald JR, Soulis ED, Kouwen N, Pietroniro A. 1995. A land cover-based snow cover representation for distributed hydrologic models. *Water Resources Research* **31**(4): 995–1009.
- Faria DA. 1998. *Distributed energetics of boreal forest snowmelt*. MSc thesis, Department of Agricultural and Bioresource Engineering, University of Saskatchewan: Saskatoon, Saskatchewan; 140 pp.
- Golding DL, Swanson RH. 1986. Snow distribution patterns in clearings and adjacent forest. *Water Resources Research* **22**: 1931–1940.
- Halliwell DH, Apps MJ. 1997. *BOReal Ecosystem–Atmosphere Study (BOREAS) Biometry and Auxiliary Sites: Overstory and Understory Data*. Natural Resources Canada, Canadian Forest Service, Northern Forestry Centre; 254 pp.
- Jones HG. 1987. Chemical dynamics of snowcover and snowmelt in a boreal forest. In *Seasonal Snowcovers: Physics, Chemistry, Hydrology*, Jones HG, Orville-Thomas WJ (eds), NATO ASI Series C211. Reidel: Dordrecht; 531–574.
- Martinez J, Rango A. 1991. Indirect evaluation of snow reserves in mountain basins. *Snow, Hydrology and Forests in High Alpine Areas*, IAHS Publication 205. International Association of Hydrological Sciences: Wallingford, 111–119.
- Martinez J, Seidel K, Burkhart U, Baumann R. 1991. Areal modelling of snow water equivalent based on remote sensing techniques. *Snow, Hydrology and Forests in High Alpine Areas*, IAHS Publication 205. International Association of Hydrological Sciences: Wallingford, 121–129.
- Metcalfe RA, Buttle JM. 1995. Controls of canopy structure on snowmelt rates in the boreal forest. *Proceedings of the Eastern Snow Conference* **52**: 249–257.
- Metcalfe RA, Buttle JM. 1998. A statistical model of spatially-distributed snowmelt rates in a boreal forest basin. *Hydrological Processes* **12**: 1701–1722.
- Ni W, Li X, Woodcock C, Roujean JL, Davis RE. 1997. Transmission of solar radiation in boreal conifer forests: measurements and models. *Journal of Geophysical Research* **102**(D24): 29555–29566.
- Pomeroy JW, Goodison BE. 1997. Winter and snow. *Surface Climates of Canada*. McGill/Queen's University Press: Kingston and Montreal.
- Pomeroy JW, Granger RJ. 1997. Sustainability of the western Canadian boreal forest under changing hydrological conditions—I—snow accumulation and ablation. In *Sustainability of Water Resources under Increasing Uncertainty*, Rosjberg D, Boutayeb N, Gustard A, Kundzewicz Z, Rasmussen P (eds), IAHS Publication 240. International Association of Hydrological Sciences Press: Wallingford; 237–242.
- Pomeroy JW, Gray DM. 1995. *Snow Accumulation, Relocation and Management*. NHRI Science Report No. 7, Environment Canada: Saskatoon, Saskatchewan; 136 pp.
- Pomeroy JW, Gray DM, Shook KR, Toth B, Essery RLH, Pietroniro A, Hedstrom N. 1998a. An evaluation of snow accumulation and ablation processes for land surface modelling. *Hydrological Processes* **12**: 2339–2367.
- Pomeroy JW, Parviainen J, Hedstrom N, Gray DM. 1998b. Coupled modelling of forest snow interception and sublimation. *Hydrological Processes* **12**: 2317–2337.
- Pomeroy JW, Davies TD, Jones HG, Marsh P, Peters NE, Tranter M. 1999. Transformations of snow chemistry in the boreal forest: accumulation and volatilisation. *Hydrological Processes* **13**: 2257–2273.
- Shook K. 1995. *Simulation of the ablation of prairie snowcovers*. PhD thesis, Department of Agricultural and Bioresource Engineering, University of Saskatchewan: Saskatoon, Saskatchewan; 189 pp.
- Shook K, Gray DM. 1997. Snowmelt resulting from advection. *Hydrological Processes* **11**: 1725–1736.
- Stedinger JR, Vogel RM, Foufoula-Georgiou E. 1993. Frequency analysis of extreme events. In *Handbook of Hydrology*, Maidment DR (ed.). McGraw-Hill; 18.1–18.66.
- Sturm M. 1992. Snow distribution and heat flow in the taiga. *Arctic and Alpine Research* **24**: 145–152.
- Takahara H, Higuchi K. 1985. Thermal modification of air moving over melting snow surfaces. *Annals of Glaciology* **6**: 235–237.
- Verry ES, Lewis JR, Brooks KN. 1983. Aspen clearcutting increases snowmelt and storm flow peaks in north central Minnesota. *Water Resources Bulletin* **19**: 59–67.
- Weisman RN. 1977. Snowmelt: a two-dimensional turbulent diffusion model. *Water Resources Research* **13**: 337–342.
- Woo M, Steer P. 1986. Monte Carlo simulation of snow depth in a forest. *Water Resources Research* **22**: 864–868.